Module 5 - Dispersion and Dispersion Mitigation

Dr. Masud Mansuripur

Chair of Optical Data Storage, University of Arizona

Dr. Masud Mansuripur is the Chair of Optical Data Storage and Professor of Optical Sciences in the University of Arizona. His areas of research include optical data storage; magneto-optics; optics of polarized light in systems of high numerical aperture; magnetic and magneto-optical properties of thin solid films; magnetization dynamics, integrated optics for optical heads (data storage systems); information theory, optical signal processing, biological data storage, erbium-doped fiber amplifiers and lasers.

Email: masud@u.arizona.edu

Introduction

A pulse of light propagating in a transparent medium may generally be considered a superposition of plane-waves of differing frequencies ω. Each such plane-wave has a phase velocity $c/n(\omega)$, specified by the refractive index of the medium at the corresponding frequency. As the pulse propagates through the medium, the frequency-dependence of the refractive index produces changes in the relative phase of the various plane-wave constituents of the pulse. This "dephasing" of the constituent plane-waves is ultimately responsible for the distortion and spreading of the pulse along the direction of propagation. In this chapter we analyze the propagation of an optical pulse in a dispersive medium and derive expressions for the group velocity, group velocity dispersion, and pulse-broadening factor.

5.1 Pulse propagation in an isotropic, homogeneous, dispersive medium.

Consider a periodic train of light pulses propagating along the z-axis in a Cartesian coordinate system. The amplitude of this pulse train is denoted by $a(t, z)$, a function of the coordinate z and time t. At the origin of the coordinates, $z = 0$, the Fourier spectrum of the pulse is given by

$$A(f) = \sum_{m=-M}^{M} A_m \, \delta(f - f_o - m\Delta f). \qquad \textit{(Equation 5.1)}$$

Here $A_m = |A_m| \exp(i\phi_m)$ is the complex amplitude of the spectral component at $f = f_o + m\Delta f$, where f_o is the central frequency of the spectrum. At $z = 0$, the pulse amplitude will be

The authors would like to acknowledge support from the National Science Foundation through CIAN NSF ERC under grant #EEC-0812072.

$$a(t, z = 0) = \Sigma\, |A_m| \cos[2\pi(\, f_o + m\Delta f\,)t - \phi_m]. \qquad \textit{(Equation 5.2)}$$

Here the time-dependence factor is assumed to be $\exp(-i2\pi f\, t)$. In the limit $\Delta f \to 0$, the above sum is replaced by an integral, and one recovers a single pulse of continuous spectrum $A(\, f\,)$. **Figure 5.1** shows plots of $A(\, f\,)$ and $a(t, z = 0)$ for the specific values of $f_o = 3.75 \times 10^{14}$Hz (corresponding to $\lambda_o = c/f_o = 0.8\ \mu m$), $\Delta f = 0.01 f_o$, and $M = 10$. The amplitude function $a(t, z = 0)$ in **Figure. 5.1** is periodic, with a period $T = 1/\Delta f \approx 267$ fs; a single period of the function is shown in **Figure. 5.1(b)**, and a close-up of the pulse appears in **Figure. 5.1(c)**.

Pulse Broadening

At any point $Z = z_o$ along the propagation path, each Fourier component in **Equation. (5.1)** will be multiplied by $\exp(i2\pi n f\, z_o/c)$, where $f = f_o + m\Delta f$ is the specific frequency for that component of the spectrum, and n is the effective refractive index of the medium; c is the speed of light in vacuum. In free-space, $n = 1.0$, and the pulse amplitude at $Z = z_o$ simply becomes $a(t, z = z_o) = a(t - z_o/c)$. The pulse then propagates at the speed of light c, without any change of shape whatsoever. In a (homogeneous and isotropic) medium of refractive index n, however, the dependence of n on the frequency f complicates the propagation process. For a sufficiently narrow spectrum, one may approximate the dependence of n on f by the first few terms of the Taylor series of $n(\, f\,)$, namely,

$$n(\, f\,) \approx n_o + n_1(\, f - f_o) + n_2(\, f - f_o)^2. \qquad \textit{(Equation 5.3)}$$

The propagation factor at $f = f_o + m\Delta f$, up to and including 2nd-order terms in $(\, f - f_o)$, may then be written as follows:

$$\exp(i2\pi n f\, z_o/c) \approx \exp(-i2\pi n_1\, f_o^2\, z_o/c)\, \exp[i2\pi(n_1 + n_2\, f_o)(\, f - f_o)^2\, z_o/c]$$

$$\times \exp[i2\pi(n_o + n_1\, f_o)\, f\, z_o/c]. \qquad \textit{(Equation 5.4)}$$

The authors would like to acknowledge support from the National Science Foundation through CIAN NSF ERC under grant #EEC-0812072.

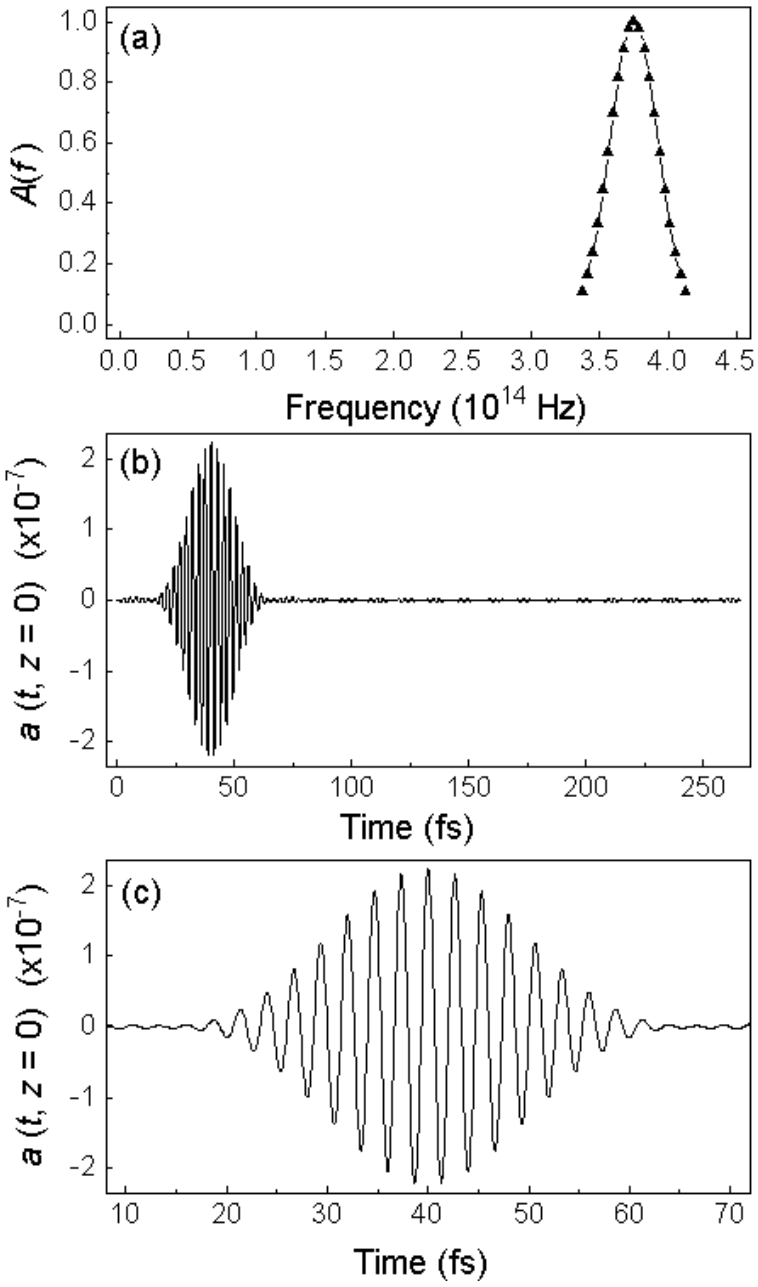

***Figure 5.1**: Amplitude A(f) of the Fourier transform of a Gaussian pulse train described by Equation. (5.1), having $f_o = 3.75 \times 10^{14}$ Hz, $\Delta f = 0.01 f_o$, and M = 10. The corresponding amplitude profile a(t, z = 0) is a periodic function of time, with period $T = 1/\Delta f \approx 267$ fs. A single period of the pulse train is shown in (b), and a close-up appears in (c).*

The authors would like to acknowledge support from the National Science Foundation through CIAN NSF ERC under grant #EEC-0812072.

In the above equation, the first term on the right-hand-side is a constant phase-factor (independent of f), which can, for purposes of the present analysis, be ignored. The second term is a quadratic phase-factor in $(f - f_o) = m\Delta f$, which may be combined with the phase ϕ_m of A_m in **Equation. (5.2)**; this term is ultimately responsible for the broadening and chirp induced on the pulse by the effects of dispersion. The last term is a linear phase-factor that translates the (dispersed) pulse from $t = 0$ at $z = 0$ to $t = (n_o + n_1 f_o) z_o/c$ at $z = z_o$. The group velocity V_g is thus found to be

$$V_g = c/(n_o + n_1 f_o). \qquad \textit{(Equation 5.5)}$$

When $n_1 = 0$, the refractive index is, to first order, independent of the optical frequency f, and the group velocity V_g would be equal to the phase velocity $V_{ph} = c/n_o$. In general, the refractive index of a *transparent* optical material is an increasing function of the frequency f, hence $n_1 \geq 0$ and $V_g \leq V_{ph}$. For a typical material such as fused silica, where $n_o = 1.46$ and $n_1 = 4.2 \times 10^{-17}$ s at $f_o = 5.4546 \times 10^{14}$ Hz (corresponding to $\lambda_o = 0.55$ μm), $V_g \approx 0.985 V_{ph}$. (For fused silica in the wavelength range $\lambda = 0.3\,\mu\text{m} - 1.6\,\mu\text{m}$, plots of n_o, n_1, n_2 versus the optical frequency f are shown in **Figure. 5.2.**)

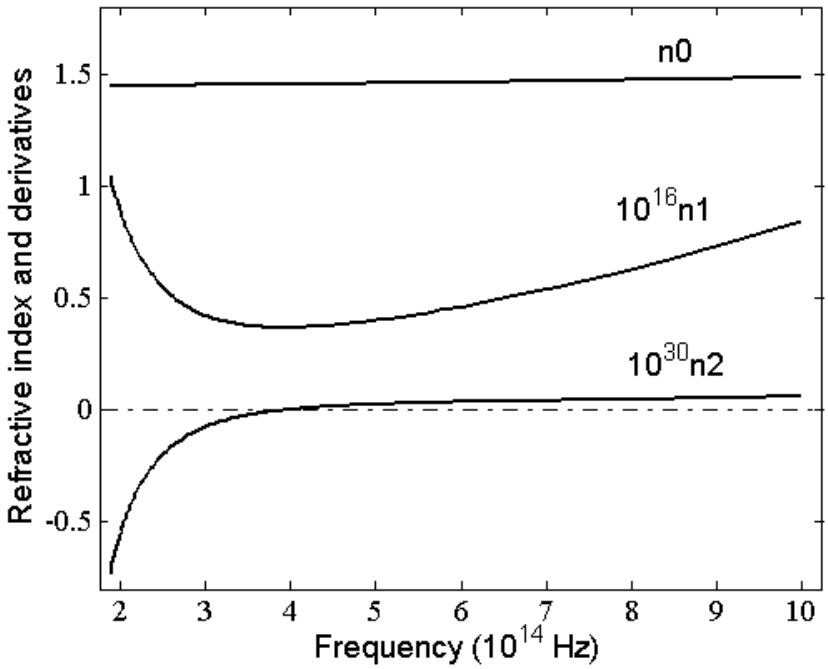

***Figure 5.2**: Plots of n_o, n_1, n_2 versus the optical frequency f for fused silica in the wavelength range $\lambda = 0.3\,\mu\text{m} - 1.6\,\mu\text{m}$. The refractive index $n_o(f)$ is measured and fitted to the Sellmeier equation, then the derivatives of the equation are obtained analytically to yield the plots of n_1 and n_2.*

The authors would like to acknowledge support from the National Science Foundation through CIAN NSF ERC under grant #EEC-0812072.

Note that the above arguments have been presented in the context of propagation in a homogeneous medium, where $n(f)$ is a characteristic of the material environment. For a beam confined to a waveguide, however, the index $n(f)$ is an effective index that depends not only on the material properties of the core and the cladding, but also on the structure of the waveguide. **Equation (5.5)** will still be applicable in this case, but the coefficients n_o and n_1 must be obtained for the effective index n_{eff} of the waveguide, for the particular mode under consideration. (See the section "*Slab waveguide and the effective refractive index of guided modes*" for a discussion of guided modes and the effective index of a simple slab waveguide.)

Figure 5.3 shows the pulse of **Figure 5.1** after propagating a distance of 4.0 mm in fused silica ($n_o = 1.4534$, $n_1 = 3.69 \times 10^{-17}$ s, $n_2 = -0.6 \times 10^{-33}$ s^2 at $\lambda_o = c/f_o = 0.8$ μm). Clearly it does not take much propagation for a short pulse of the given wavelength in the given material to become significantly broadened.

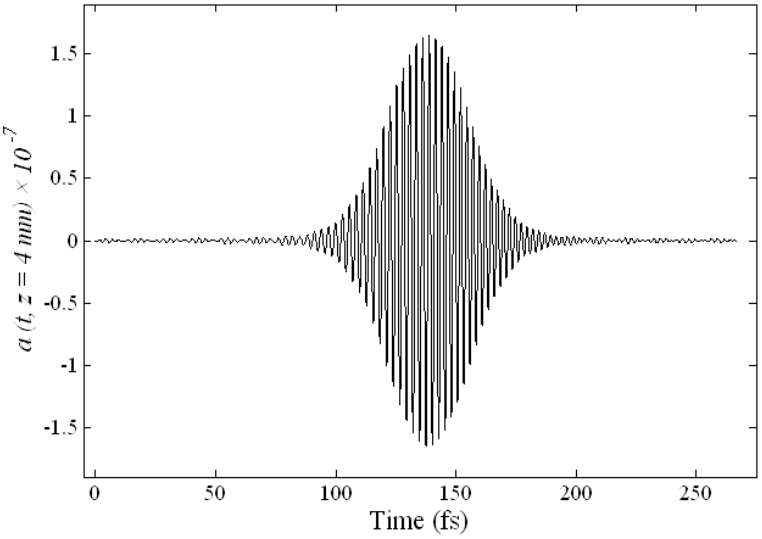

***Figure 5.3**: The pulse depicted in Figure. 1 after propagating a distance of 4.0 mm in fused silica ($n_o = 1.4534$, $n_1 = 3.69 \times 10^{-17}$ s, $n_2 = -0.6 \times 10^{-33}$ s^2 at $\lambda_o = c/f_o = 0.8$ μm).*

Group velocity dispersion

The group velocity defined by **Equation. (5.5)** may itself be treated as a function of frequency, namely, $V_g(f) = c/(n + n'f)$, where n' is the derivative of n with respect to f. The variations of V_g in the vicinity of a given frequency f_o may then be analyzed in terms of the derivative of V_g with respect to f, evaluated at $f = f_o$, namely,

$$V_g'(f_o) = -2c(n_1 + n_2 f_o)/(n_o + n_1 f_o)^2. \qquad \textit{(Equation 5.6)}$$

The authors would like to acknowledge support from the National Science Foundation through CIAN NSF ERC under grant #EEC-0812072.

(Here we have used the fact that $n'' = 2n_2$.) The so called *group velocity dispersion* (GVD) defined by **Equation. (5.6)** is clearly proportional to the coefficient $(n_1 + n_2 f_o)$ appearing in the quadratic phase factor in **Equation. (5.4)**. In particular, the sign of $(n_1 + n_2 f_o)$ determines whether V_g is an increasing or decreasing function of frequency.

The spectral amplitude $A(f)$ of a single light pulse may be a Gaussian function of frequency f, namely,

$$A(f) = A_o \exp[-\pi\alpha(f - f_o)^2], \qquad \textit{(Equation 5.7)}$$

where A_o and α are two complex constants. Whereas $A_o = |A_o|\exp(i\phi_o)$ may be chosen arbitrarily, the parameter $\alpha = \alpha_1 - i\alpha_2$ is required to have a positive real part, that is, $\alpha_1 > 0$. The units of A_o are volt·second/meter, while α has units of sec^2. The Fourier transform of $A(f)$ is given by

$$\begin{aligned} a(t) &= \text{Real}\,\{A_o\alpha^{-1/2}\exp(-\pi t^2/\alpha)\exp(-i\,2\pi f_o t)\} \\ &= |A_o|\,(\alpha_1^2 + \alpha_2^2)^{-1/4}\exp\{-\pi[\alpha_1/(\alpha_1^2 + \alpha_2^2)]t^2\} \\ &\qquad \times \cos\{2\pi f_o t + \pi[\alpha_2/(\alpha_1^2 + \alpha_2^2)]\,t^2 - \tfrac{1}{2}\tan^{-1}(\alpha_2/\alpha_1) - \phi_o\}. \end{aligned} \qquad \textit{(Equation 5.8)}$$

Note that the field amplitude $a(t)$ has units of volt/meter, namely, those of the electric field in the MKSA system of units. The pulse envelope is a Gaussian function whose width is proportional to $\sqrt{(\alpha_1^2 + \alpha_2^2)/\alpha_1}$. [To obtain the pulse's full width at half-maximum intensity (FWHM), multiply this parameter with $\sqrt{2\ln 2/\pi} \approx 0.665$.] Thus the quadratic phase-factor, having a coefficient $\pi\alpha_2$ in the exponent of the spectral function $A(f)$, causes a broadening of the pulse. For example, the coefficient of the quadratic phase-factor in **Equation (5.4)**, $\alpha_2 = 2(n_1 + n_2 f_o)z_o/c$, indicates a growing pulse-width with the propagation distance z_o. The time-dependent chirp frequency in **Equation (5.8)**, $f = f_o + [\alpha_2/(\alpha_1^2 + \alpha_2^2)]t$, varies continuously along the pulse within a range centered at f_o (noting that the pulse of **Equation (5.8)** is centered at $t = 0$). If $(n_1 + n_2 f_o)$ happens to be positive, then the chirp frequency will increase with time (up-chirp). Since the GVD, given by **Equation (5.6)**, is negative in this case, the leading edge of the pulse, having a frequency that is lower than f_o, travels faster than the trailing edge, which has a higher frequency. On the other hand, if $(n_1 + n_2 f_o)$ happens to be negative, the chirp frequency will decrease with time (down-chirp). However, since the GVD is positive in this case, the leading edge, once again, will travel faster than the trailing edge. Either way, the pulse is seen to broaden as a result of propagation in the dispersive medium, which is the same conclusion arrived at earlier, when we argued that the width of the Gaussian pulse of **Equation (5.8)** is an increasing function of α_2. The minimum width occurs at $z_o = 0$, where $\alpha_2 = 0$; here the pulse is said to be *transform-limited*, meaning that its width, $\sqrt{\alpha_1}$, cannot be reduced any further, owing to the finite width of its Fourier transform $A(f)$.

The authors would like to acknowledge support from the National Science Foundation through CIAN NSF ERC under grant #EEC-0812072.

5.2 Dispersion mitigation in optical fibers

The term "chromatic dispersion" for a transparent medium refers to the phenomenon that the phase velocity and group velocity of light propagating in the medium depend on the optical frequency ω (or, equivalently, on the wavelength λ). A related quantitative measure is the group velocity dispersion. The attribute "chromatic" is used to distinguish this type of dispersion from other types, which are relevant in optical fibers, namely, polarization mode dispersion (PMD), and modal dispersion (MD) in multi-mode fibers. One often distinguishes normal dispersion from anomalous dispersion. Normal dispersion, where the group velocity decreases with increasing optical frequency, occurs for most transparent media in the visible spectral region. Anomalous dispersion sometimes occurs at longer wavelengths, e.g., in silica glass for wavelengths longer than its zero-dispersion wavelength of $\lambda \sim 1.3\,\mu\text{m}$.

Dispersion compensation essentially means canceling the chromatic dispersion of an optical element or system. However, the term is often used in a more general sense of "dispersion management," which is the control of the chromatic dispersion of a given system to mitigate its undesirable effects. Dispersion mitigation entails adding optical elements with a suitable amount of dispersion, with the goal of avoiding excessive temporal broadening and/or distortion of short light pulses. Dispersion compensation may be provided with sections of differently-designed fiber, or with compensation modules containing dispersion-shifted fibers or chirped fiber Bragg gratings (FBGs). The latter have the advantage of compactness and low insertion loss. The required dispersion of the compensating element(s) may be normal or anomalous.

In optical fiber communication, chromatic dispersion is generally specified by the dispersion parameter $D_\lambda = -(2\pi c/\lambda^2)\partial^2 k/\partial\omega^2$ in units of ps/nm/ km. Between wavelength bands with normal and anomalous dispersion, there is a zero-dispersion wavelength. Third and higher-order dispersion, caused by high-order derivatives $\partial^n k/\partial\omega^n$, produce more complicated changes in the pulse shape. A challenge in dispersion compensation is to combat not only the lowest (i.e., second) order dispersion, but also to eliminate these higher orders in order to approach transform-limited pulse shapes. When dealing with very broad optical spectra, one sometimes has to combat 3rd, 4th, 5th and even 6th order dispersion.

In optical fiber communication, dispersion compensation modules (DCMs) are used to mitigate the chromatic dispersion of a long span of transmission fiber. Typically, such a module provides a fixed amount of dispersion, although tunable DCMs are also available. A DCM with its own input/output fiber connectors can be readily inserted into a fiber-optic link. The insertion losses may be compensated, for example, with an erbium-doped fiber amplifier (EDFA) in a $1.5\,\mu\text{m}$ telecommunication system; DCMs are often placed between two fiber amplifiers.

The authors would like to acknowledge support from the National Science Foundation through CIAN NSF ERC under grant #EEC-0812072.

Dispersion compensation modules based on several different technologies are commercially available. A frequently used method employs a long piece of dispersion-shifted fiber wound up around a spool of 10-20 cm diameter. The fiber, for example, may be optimized to provide compensating dispersion for a 100 km span of a transmission fiber, while introducing an optical loss of only a few decibels. A more compact device, often with lower insertion loss, uses a chirped fiber Bragg grating. A large amount of dispersion can be compensated with relatively long FBGs (possibly tens of centimeters in length). The dispersion can be tuned by varying the FBG's temperature with built-in controllers.

A central aspect of DCM design, of course, is the amount of chromatic dispersion provided, which depends on the type and length of the transmission fiber that needs to be compensated. For example, dispersion-shifted transmission fibers require much less compensation. The dispersion slope, which is related to higher-order dispersion, can strongly limit the usable bandwidth, which is important particularly in the case of wavelength division multiplexing (WDM) systems. Depending on the type of transmission fiber, different relative dispersion slopes are required, with larger dispersion slopes making the DCM design more challenging.

Dispersion-shifted fiber

A dispersion-shifted fiber is one with a non-standard zero-dispersion wavelength. Standard silica fibers exhibit zero chromatic dispersion in the 1.3 μm wavelength region. This was convenient for early optical fiber communications systems, which operated around 1310 nm. However, the 1.5 μm region has gained far more significance in recent years, because of lower optical losses, and also because erbium-doped fiber amplifiers (EDFAs) have become available for this region. (The 1.3 μm amplifiers do not reach comparable performance.) In the 1.5 μm region, however, dispersion-unshifted SMFs exhibit significant anomalous dispersion. This can be a problem for linear transmission, because it leads to significant pulse broadening, limiting the achievable transmission rate over long distances. Therefore, dispersion-shifted fibers with modified waveguide dispersion have been developed, so as to shift the zero-dispersion wavelength into the 1.5 μm region. This is achieved by modifying the refractive index profile of the core. Common index profiles of dispersion-shifted fibers have a triangular, trapezoidal or Gaussian shape.

Zero chromatic dispersion is not necessarily desirable, particularly in multiple-channel transmission over a single fiber, where four-wave mixing effects can, in the absence of dispersion, result in phase-matching and, subsequently, significant distortions of the light pulse. Therefore, it is sometimes advantageous to use non-zero dispersion-shifted fibers, designed to have a weak dispersion within the wavelength range of interest for data transmission, with the zero-dispersion wavelength lying just outside this region. There are also dispersion-flattened fibers with a fairly constant group delay dispersion over some wavelength range, i.e., low higher-order dispersion. They can, for example, exhibit near-zero-dispersion in the telecom C band. Such fibers are important for data transmission with wavelength division multiplexing (WDM).

The authors would like to acknowledge support from the National Science Foundation through CIAN NSF ERC under grant #EEC-0812072.

They often have a W-shaped profile of the refractive index, although profiles with a graded-index and multiple steps have also been developed.

Fiber Bragg Grating

A fiber Bragg grating (FBG) is a reflective structures in the core of an optical fiber with a periodic or aperiodic perturbation of the effective refractive index, as shown in **Figure 5.4**. Typically, the index perturbation is periodic over a length of several millimeters or centimeters, and the period is a fraction of a micron.

***Figure 5.4**: Schematic of a fiber Bragg grating. The core has a periodically varying refractive index over some length. Typical dimensions are 8μm core and 125μm cladding diameters. Periods of the refractive index modulation vary from hundreds of nanometers for conventional FBGs to hundreds of microns for long-period gratings.*

The refractive index perturbation leads to the reflection of light propagating along the fiber in a narrow range of wavelengths for which the Bragg condition $2\pi/\Lambda = 2(2\pi n_{\text{eff}}/\lambda)$ is satisfied. Here Λ is the grating period, n_{eff} is the effective refractive index of light in the fiber, and λ is the vacuum wavelength. The strongly reflected wavelength is thus $\lambda = 2n_{\text{eff}}/\Lambda$. The above condition implies that the wavenumber of the grating matches the difference of the (opposite) wave-vectors of the incident and reflected waves. In that case, the complex amplitudes corresponding to reflected field contributions from different parts of the grating, all being in phase, add up constructively. Even a weak index modulation with a magnitude of, say, $\Delta n/n \sim 10^{-4}$ is sufficient for achieving nearly total reflection, provided the grating is long enough (e.g., a few millimeters in this case). Light at other wavelengths which do not satisfy the Bragg condition is essentially unaffected by the FBG. The reflection bandwidth of an FBG, typically below 1nm, depends on the length of the grating as well as the strength of the index modulation. The narrowest bandwidths are obtained for long gratings with weak index modulation. Large bandwidths may be achieved with short and strong gratings, but also with aperiodic designs.

The authors would like to acknowledge support from the National Science Foundation through CIAN NSF ERC under grant #EEC-0812072.

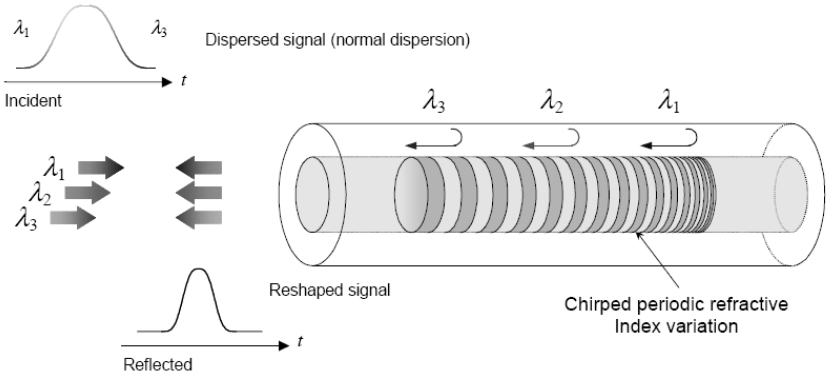

***Figure 5.5**: A chirped FBG compensates for dispersion by reflecting different wavelengths at different locations along the grating.*

As the wavelength of maximum reflectivity depends not only on the grating period but also on temperature and mechanical strain, FBGs can be used as temperature and strain sensors. Transverse stress, as generated, for example, by squeezing a fiber grating between two flat plates, induces birefringence and thus polarization-dependent Bragg wavelengths.

For multimode fibers, a multitude of core modes has to be accounted for. In such cases, the coupling coefficients depend not only on the amplitude of the index modulation, but also on the three-dimensional shape of the grating. Also, the wavelength of maximum reflection can differ for different modes, as the Bragg condition is influenced by the different propagation constants.

If the strength of the index modulation in a grating is constant over some length, and suddenly drops to zero outside that range, the reflection spectrum exhibits side-lobes, especially if the peak reflectivity is high. These side-lobes could be disturbing, for instance, when the FBG is used as an optical filter. The side-lobes can be largely removed with the technique of apodization, where the index modulation is smoothly ramped up and down along the grating.

Fiber gratings with a periodic index modulation can have interesting properties, such as reflectivity curves without side-lobes, multiple tailored reflection bands, or special chromatic dispersion profiles. Particularly for dispersion compensation, so-called chirped fiber gratings are used, where the Bragg wavelength varies with position along the grating. It is possible to achieve very large group delay dispersion in a short length of fiber, sufficient for compensating the dispersion of a long span of transmission fibers in an optical communication system.

Fabrication of FBGs typically involves the illumination of the core material with ultraviolet laser light, which induces structural change and thus a permanent modification of the refractive index. The photosensitivity of the core glass is actually strongly dependent on the chemical composition and the UV wavelength: whereas the photosensitivity of silica glass is weak, germanosilicate glasses exhibit a strong effect, making index contrasts as large as $\Delta n/n \sim 10^{-3}$ possible. The first

The authors would like to acknowledge support from the National Science Foundation through CIAN NSF ERC under grant #EEC-0812072.

FBGs were fabricated with a visible laser beam propagating along the fiber core, but a more versatile technique was soon developed based on the interferometric superposition of ultraviolet beams arriving from the side of the fiber (transverse holographic technique). The angle between the UV beams determines the period of the interference pattern in the fiber core and thus the Bragg wavelength Λ. The two UV beams are often generated by exposing a periodic phase mask with a single UV beam (phase mask technique), using the two first-order diffracted beams. Non-periodic phase masks can be used to obtain more complicated patterns. In the point-by-point technique, regions with increased refractive index are written sequentially with a sharply focused laser beam. This is an appropriate and flexible technique particularly for long-period gratings.

Instead of ultraviolet light, infrared light in the form of intense femtosecond pulses can also be used for writing Bragg gratings in various kinds of glasses. In that case, two-photon absorption occurs near the focus of the laser beam, but not in regions outside the focus. It is even possible to write such gratings through the polymer coating of a fiber, since the intensity in the coating is much lower when the beam is focused on the fiber core.

5.3 Polarization mode dispersion

Polarization mode dispersion (PMD) is a form of modal dispersion where two different polarizations of light in a waveguide, which normally travel at the same speed, travel at different speeds due to imperfections and asymmetries, causing random spreading of optical pulses. A related effect is polarization-dependent loss (PDL), in which the two polarization states suffer different rates of loss in the fiber due, again, to asymmetries. Unless these effects are eliminated or compensated, they ultimately limit the rate at which data can be transmitted over a fiber.

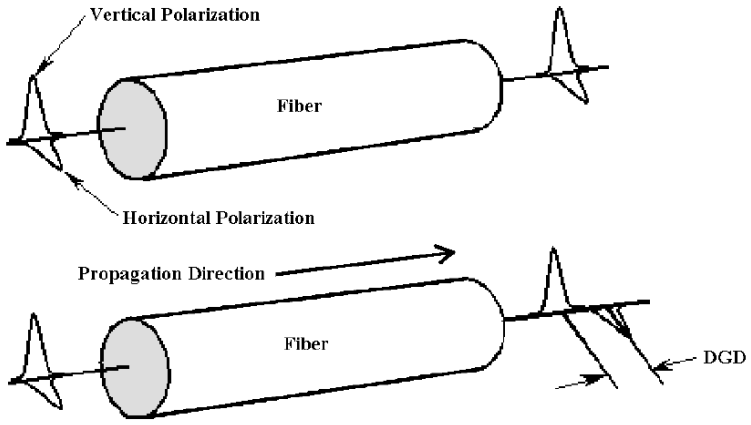

***Figure 5.6**: (Top) There is no PMD in a perfect optical fiber. (Bottom) Real fibers have random core asymmetries and are subject to stresses that give rise to differential group delay (DGD). Geometric asymmetries or mechanically-induced birefringence create fast and slow axes along the fiber. Consequently, one polarization mode travels*

The authors would like to acknowledge support from the National Science Foundation through CIAN NSF ERC under grant #EEC-0812072.

faster than the other, resulting in a propagation time difference between the two modes, commonly referred to as DGD and measured in picoseconds.

Polarization Dependent Loss

In an ideal optical fiber, where the core has a perfectly circular cross-section, the fundamental mode has two orthogonal polarizations (defined as the orientation of the *E*-field) that travel at the same speed. The signal propagating along the length of the fiber is a random superposition of these two polarizations, which is inconsequential in an ideal fiber because the two polarization modes, being degenerate, propagate identically. The imperfections of a realistic fiber, however, break the circular symmetry, causing the two polarizations to propagate with different speeds. The two polarization components of a signal thus slowly separate, causing individual pulses to spread and adjacent pulses to overlap. Because the imperfections are random, the pulse spreading effects correspond to a random walk, and thus have a mean polarization-dependent time-differential, or differential group delay, $\Delta\tau$, proportional to the square root of the propagation distance *L*. Defining D_{PMD} as a parameter of the fiber that measures the strength and frequency of imperfections (units = ps/$\sqrt{}$km), we may write $\Delta\tau = D_{\text{PMD}}\sqrt{L}$.

The symmetry-breaking random imperfections fall into several categories. First, there is geometric asymmetry, e.g., slightly elliptical cores. Also, there are stress-induced material birefringences, in which the refractive index itself depends on the polarization. Both of these effects can stem from either imperfection in manufacturing or from thermal and mechanical stresses imposed on the fiber in the field; moreover, the latter stresses generally vary over time.

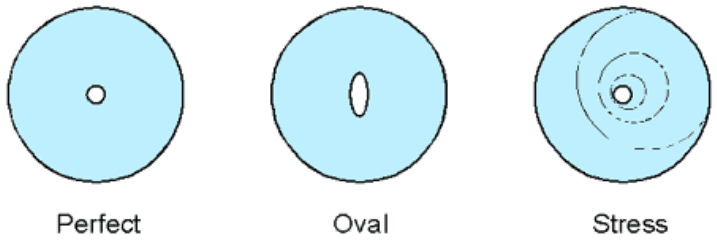

***Figure 5.7**: Cross-sections of an optical fiber. A major cause of PMD is the asymmetry of the fiber-optic strand, which is the case, for example, when the fiber has an elliptical core. The asymmetry may be inherent in the fiber from the manufacturing process, or it may be a result of mechanical stress on the deployed fiber. While the inherent asymmetries are fairly constant over time, the mechanical stress due to movement of the fiber can vary, resulting in dynamic PMD. Roughly 20 to 30% of the SMFs manufactured before the mid 1990s had imperfectly round cores. This defect became a problem as the data-rates and span-lengths of fiber-optic networks increased over the years. Of course, no fiber's core is perfectly symmetric, but the older fibers are sufficiently asymmetric to produce enough PMD to render the transmitted signal undetectable.*

The authors would like to acknowledge support from the National Science Foundation through CIAN NSF ERC under grant #EEC-0812072.

Polarization Mode Disperation Compensation

PMD is the major challenge facing system developers as they attempt to deploy 40Gb/s optical networks, although deleterious effects of PMD have been evident in 10Gb/s networks as well. While most other fiber distortions and nonlinearities are relatively stable over time, PMD poses new challenges because of its instability and variations with time. A possible solution to the problem would be to use a polarization maintaining fiber, whose symmetry is so strongly broken (e.g., via a highly elliptical core) that an input polarization along a principal axis is maintained all along the fiber; the second polarization mode is never excited, and, therefore, PMD does not occur. Polarization-maintaining fibers, however, are not currently favored for this application due to their relatively high losses and higher cost.

A PMD compensation device used in practice splits the output of the transmission line into two principal polarizations – usually those with $d\tau/d\omega \approx 0$, i.e., no first-order variation of time-delay with frequency – and applies a differential delay to re-synchronize the two components. The random, time-dependent nature of PMD requires an active device that responds to feedback over time, thus making PMD compensation expensive and complex.

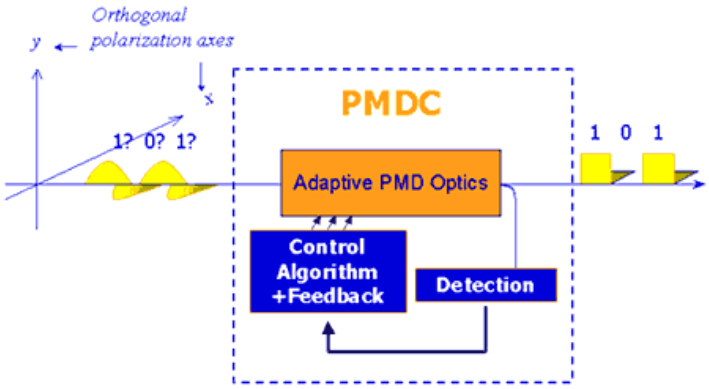

Figure 5.8: *Graphical representation of PMD compensation on a distorted optical pulse, where the dispersed optical bits emerging from the fiber network are corrected. Before correction, the polarized pulses of the bits are separated and dispersed by PMD. The compensator realigns and reshapes the pulses so they can be correctly decoded by the receiver. The process usually involves applying some sort of stress to a fiber at one or more points to modify the polarization state of the optical signal. The adaptive optics of the compensator are controlled by an intelligent algorithm driven by analysis of the optical bits. The significant variability of PMD as function of wavelength within a transmission band requires that compensation be performed on a per-wavelength basis.*

The authors would like to acknowledge support from the National Science Foundation through CIAN NSF ERC under grant #EEC-0812072.

References

1. I. A. Walmsley *et al*, "The role of dispersion in ultrafast optics", Rev. Sci. Instrum. **72**, 1 (2001).

2. N. M. Litchinitser *et al*, "Fiber-based tunable dispersion compensation", J. Opt. Fiber Comm. Rep. **4**, 41 (2007).

3. R. Jones *et al*, "Silicon photonic tunable optical dispersion compensator", Opt. Express **15**, 15836 (2007).

4. G. Meltz, *et al*, "Formation of Bragg gratings in optical fibers by a transverse holographic method," *Opt. Lett.* **14**, 823 (1989).

5. J. Canning, *Fibre Gratings and Devices for Sensors and Lasers, Lasers and Photonics Reviews*, **2**, 275-289, Wiley, New York (2008).

6. A. Othonos and K. Kalli, *Fiber Bragg Gratings*: *Fundamentals and Applications in Telecommunications and Sensing*, Artech House (1999).

7. J. N. Damask, *Polarization Optics in Telecommunications*, Springer, New York (2004).

8. L. Xu, S. X. Wang, H. Miao, and A. M. Weiner, "Polarization mode dispersion spectrum measurement via high-speed wavelength-parallel polarimetry," Appl. Opt. **48**, 4688-97 (2009).

†Parts of this chapter have been adapted from available resources on the internet, such as *www.rp-photonics.com*, *en.wikipedia.org*, and *www.iec.org*.

The authors would like to acknowledge support from the National Science Foundation through CIAN NSF ERC under grant #EEC-0812072.